HHS Public Access

Author manuscript

Life Sci. Author manuscript; available in PMC 2019 December 18.

Published in final edited form as:

Life Sci. 2019 March 15; 221: 1–12. doi:10.1016/j.lfs.2019.02.014.

Exchange protein directly activated by cAMP plays a critical role in regulation of vascular fibrinolysis

Xi He[a,b], **Aleksandra Drelich**[a], **Shangyi Yu**[a,b], **Qing Chang**[a], **Dejun Gong**[b], **Yixuan Zhou**[b], **Yue Qu**[a], **Yang Yuan**[b], **Zhengchen Su**[a], **Yuan Qiu**[c], **Shao-Jun Tang**[d], **Angelo Gaitas**[e], **Thomas Ksiazek**[a], **Zhiyun Xu**[b], **Jia Zhou**[f], **Zongdi Feng**[g], **Maki Wakamiya**[h], **Fanglin Lu**[b,*], **Bin Gong**[a,*]

[a]Department of Pathology, University of Texas Medical Branch, Galveston, TX 77555, USA

[b]Department of Cardiovascular Surgery, Changhai Hospital, Shanghai 200433, China

[c]Department of Mathematics and Statistics, Texas Tech University, Lubbock, TX 79409, USA

[d]Department of Neuroscience and Cell Biology, University of Texas Medical Branch, Galveston, TX 77555, USA

[e]Department of Neurology, Icahn School of Medicine at Mount Sinai, NY 10029, USA

[f]Department of Pharmacology and Toxicology, University of Texas Medical Branch, Galveston, TX 77555, USA

[g]Center for Vaccines and Immunity, The Research Institute at Nationwide Children's Hospital, Columbus, OH 43205, USA

[h]Department of Neurology, University of Texas Medical Branch, Galveston, TX 77555, USA

Abstract

Plasmin-mediated fibrinolysis at the surface of vascular endothelial cells (SVEC) plays a key role in maintaining vascular hemostasis, in which the cAMP pathway participates. After externalization to the SVEC, annexin A2 (ANXA2) serves as a platform for conversion of plasminogen to plasmin. Here we describe a regulatory role of the exchange protein directly activated by cAMP (EPAC) in ANXA2 externalization and vascular fibrinolysis. Knockout of *EPAC1* in mice results in a decreased ANXA2 expression on the SVEC associated with increased fibrin deposition and fibrinolytic dysfunction. Reduced levels of EPAC1 are also found in endocardial tissues beneath atrial mural thrombi in patients. Notably, administration of recombinant ANXA2 ameliorates fibrinolytic dysfunction in the *EPAC1*-null mice. Mechanistically, EPAC1 regulates the SVEC

*Corresponding authors. lufanglin@smmu.edu.cn (F. Lu), bigong@utmb.edu (B. Gong).

Authorship contributions

B.G. and F.L. designed the study, performed experiments, analyzed data, and wrote the manuscript. F.L. and Z.X. contributed clinical samples, clinical correlative information, and performed partial *in vivo* experiments and all clinical samples-relevant experiments. X.H. and A.D. performed experiments, analyzed data, and wrote the initial draft of the manuscript. S.Y., Q.C., D.G., Y.Z., Y.Q., Y.Y., and Z.S. performed experiments and analyzed data. Y.Q. and A.G. analyzed data. S.J.T., T.K., J.Z., and Z.F. assisted in designing experiments and provided comments and editorial changes. M.W. performed experiments, analyzed data, and provided comments and editorial changes.

Disclosure of conflicts of interest

The authors declare that they have no conflicts of interests.

Appendix A. Supplementary data

Supplementary data to this article can be found online at https://doi.org/10.1016/j.lfs.2019.02.014.

plasminogen conversion depended on ANXA2. EPAC1 promotes tyrosine-23 phosphorylation of ANXA2, a prerequisite for its recruitment to the SVEC. Our data thus reveal a novel regulatory role for EPAC1 in vascular fibrinolysis.

Keywords

EPAC1; Vascular endothelial fibrinolysis; Annexin A2; Thrombosis; Atomic force microscopy

1. Introduction

Vascular endothelial cells (ECs) constitute the inner cellular lining of the vascular luminal wall, a highly dynamic and multi-functional interface between the inner vascular surface and flowing blood [1–4]. To maintain vascular patency, ECs finely orchestrate the balance between blood coagulation and fibrinolysis on their luminal surfaces *via* complicated mechanisms, of which the plasmin-based fibrinolytic system has been well characterized [5–8]. Fibrinolysis is elicited by the conversion of plasminogen to plasmin, which is activated by either of two plasminogen activators (PAs), tissue PA (tPA) or urokinase, on the surface of the fibrin thrombus or cell [5,6,9]. Plasminogen is the pro-enzyme of the principal fibrinolytic protease plasmin, which is generated upon cleavage of plasminogen by PA at a single peptide bond at position Arg_{560} – Val_{561} [10]. Besides secreting tPA on their surface, ECs express abundant plasminogen- and tPA-binding receptors [7], among which the annexin A2 (ANXA2) complex with S100A10 [$(ANXA2\text{-}S100A10)_2$] is the best recognized and is emerging as the focus of research on a growing spectrum of biologic and pathologic processes [9,11–13]. On the endothelial luminal surface, $(ANXA2\text{-}S100A10)_2$ recruits plasminogen and tPA, resulting in enhanced activation of plasminogen by at least 12-fold above baseline to produce fibrinolytic activity [9,11–13]. Moreover, *ANXA2*-null mice [14] and *S10010A*-null mice [8] both demonstrate excessive accumulation of fibrin in the microvasculature.

ANXA2 is a Ca^{2+}-regulated and phospholipid-binding protein that associates with biological membranes and the actin cytoskeleton [11,15,16]. One of the well-recognized features of ANXA2 is its capacity to interact with its binding partner S100A10 and form the so-called heterotetrameric complex $(ANXA2\text{-}S100A10)_2$, consisting of one S100A10 dimer and two ANXA2 molecules [12,17–19]. S100A10 is unique among the S100 protein family since it is locked in a permanent open conformation, which is comparable to the Ca^{2+}-bound configuration of other members [11]. The ratio of monomeric ANXA2 to $(ANXA2\text{-}S100A10)_2$ can vary among different cell types. In ECs, depletion of cellular ANXA2 results in rapid polyubiquitination of S100A10 for degradation in a proteasome [17]. ANXA2 can associate with the cellular membrane by itself [20], yet, by binding S100A10, ANXA2 increases its sensitivity to Ca^{2+} and enhances its capability to bind the cellular membrane [21] and submembranous F-actin. ANXA2 and S100A10 are predominantly detected in cytoplasm and translocate across the cell membrane by an as yet unknown mechanism, which is independent from the classic endoplasmic reticulum—Golgi pathway [22]. It has been proposed that ANXA2-containing multivesicular endosomes fuse directly with the cell membrane resulting in cell surface translocation [23]. The process is regulated distinctively

by phosphorylation of ANXA2 at different residues in its N-terminus in response to various stimuli [22,24,25]. Therefore, the dynamics of ANXA2 in and near the plasma membrane compartment can govern vascular fibrinolysis on the endothelial surface in response to various signals [11,12,21]. However, little is known about the precise mechanism mediating the cross-talk between environmental signals and the regulation of the dynamics of ANXA2 in a cell.

Cyclic adenosine monophosphate (cAMP) is an important molecular switch that translates environmental signals into regulatory effects in a cell [26–30]. In multicellular eukaryotic organisms, the effects of cAMP are transduced by two ubiquitously-expressed intracellular cAMP receptors, the classic cAMP-dependent protein kinase A (PKA), and the more recently discovered exchange protein directly activated by cAMP (EPAC) [31,32]. To date, two isoforms of EPAC, EPAC1 and EPAC2, have been identified in humans. They are encoded by independent genes and predominantly expressed in different cell types. Both EPAC isoforms function by responding to increased intracellular cAMP levels in a PKA-independent manner and act on the same immediate downstream effectors, the small G proteins Rap1 and Rap2 [33,34]. Based on accumulating evidence [35–38], the cAMP-EPAC signaling axis has been linked to vascular endothelial physiology and pathophysiology, including endothelial barrier function [1,39–43], endothelial response to inflammatory stimuli [44–46], angiogenesis [47,48], leukocyte adhesion to and migration across the endothelium [49–51], and intra-endothelial pathogen infection [52]. Indeed, pharmacological and molecular approaches using human umbilical vein endothelial cells (HUVECs) have shown that EPAC1 is the major isoform in the ECs, and that Rap activation by EPAC1, and not by EPAC2, contributes to the effects of cAMP-elevating hormones on endothelial barrier functions [1,43,53]. Of note, in ECs it has been documented that cAMP and EPAC are involved in hemostasis by driving the expressions of tPA and von Willebrand factor (vWF) [25,54,55]. Recent reports showed that, in primary human ECs, $(ANXA2\text{-}S100A10)_2$ is involved in the forskolin-induced cAMP-dependent secretion of vWF [25]. Moreover, the Epac-Rap1 pathway, which can be suppressed by EPAC specific inhibitors [56,57] can regulate exocytosis of the exocytotic organelles called Weibel-Palade bodies (WPBs), in which vWF is stored [55]. These findings prompted us to determine whether the cAMP-EPAC signaling axis plays a role in balancing blood coagulation and fibrinolysis on the vascular interior wall surface.

In the present study, by taking advantage of *EPAC1*-null mice and an EPAC-specific inhibitor, we demonstrate that EPAC1 plays a novel important role in maintaining vascular patency. Using biochemical and biomechanical assays, we found that EPAC1 exerts its regulation on vascular fibrinolysis *via* modulating endothelial surface expression of ANXA2 and its association with S100A10.

2. Methods

In four cases of rheumatic mitral stenosis with chronic atrial fibrillation, left atrial mural thrombi were seen in the left atrial appendages during open heart surgeries for mitral valve replacements under extracorporeal circulation support at Changhai Hospital, the Second Military Medical University (Shanghai, China). After removing the thrombus, a 5×5 mm^2

piece of endocardial tissue directly underneath the thrombus in the left atrial appendage was harvested. Tissue samples were flash frozen in liquid nitrogen and homogenized for immunoblotting assays by pulverizer (Spectrum Laboratories, Rancho Dominiquez, CA) as described previously [58]. The biopsy incision was closed with a 5–0 polypropylene suture. Similar tissue samples from normal donor hearts were used as normal controls. Informed written consent was obtained from each patient prior to study enrollment. This study was approved by the Committee on Ethics of Changhai Hospital.

All other methods are in the supplementary materials.

2.1. Statistics

Statistical significance was determined using Student's *t*-test or oneway analysis of variance. Results were regarded as significant if two-tailed P values were < 0.05. All data are expressed as mean ± standard error of the mean.

3. Results

3.1. Absence of the EPAC1 gene results in fibrin accumulation in the microvasculature

To ascertain the role of EPAC1 *in vivo*, we generated *EPAC1*-null mice that carry the *Rapgef3* (also known as *EPAC1*) allele lacking exons 3–6 (Fig. S1A). We confirmed that the mutant allele is null by Western immunoblotting analysis (WB) (Fig. S1B). Similar to published models [59,60], our *EPAC1*-null mice are viable, fertile, and without overt abnormalities.

In vitro evidence suggests that EPAC1 controls vascular endothelial (VE)-cadherin-mediated cell junction formation [39–41]. Given that an *in vivo* study showing that deletion of *EPAC1* inhibits endothelial barrier baseline in skin and intestine, but not heart [59], we assessed vascular integrity in brain and lung in our *EPAC1*-null model. Compared to wild-type mice, the Evans blue assay revealed no differences in the baseline of extravascular dye in brain and lung parenchyma in *EPAC1*-null mice (Fig. S2A); immunofluorescent microscopy (IF) analysis displayed similar structures of vascular tight or adherens junctions (Fig. S2B).

Excessive accumulation of intra- and extravascular fibrin is a hallmark of enhanced blood coagulation or incomplete fibrinolytic function caused by plasminogen or plasminogen activator deficiency in mice [8,14]. We employed immunohistochemistry (IHC) and IF to measure fibrin levels in tissues collected from *EPAC1*-null and wild-type mice after extensive perfusion *in vivo*. Increased fibrin signals were detected within brain, lung, and renal blood vessels in *EPAC1*-null mice, while comparable staining was not detected in similar tissues from wild-type mice (Figs. 1A,B,E,F,I,J and S3). Dual-target IF study revealed that enhanced signals of fibrin colocalized with vWF in *EPAC1*-null mice (Fig. 1M). WB analysis displayed an increased level of fibrin within tissues of lung and kidney in *EPAC1*-null mice compared to wild-type mice (Fig. 1N). Interestingly, IHC studies on tissues from wild-type mice treated with a small molecule EPAC-specific inhibitor, ESI09 (10 mg/kg/day, given intraperitoneally for 5 days) [56], recapitulated IHC findings in the *EPAC1*-null mice. Increased fibrin immunostaining within tissues of multiple organs was evident (Fig. 1C,D,G,H,K,L). A similar phenomenon was not observed in wild-type mice

treated with vehicle only. These data suggest that EPAC1 deficiency causes fibrin accumulation in a subset of tissues.

We next examined blood coagulation parameters in *EPAC1*-null mice to determine whether fibrin accumulation is caused by enhanced blood coagulation. Prothrombin time (PT) and activated partial thromboplastin time (aPTT) are two biochemical indicators of blood coagulation [8]. We observed that there were similar values of PT and aPTT between wild-type and *EPAC1*-null mice (Fig. S4A), suggesting that EPAC1 depletion does not affect the blood coagulation pathway characterized by these two assays. We also examined the platelet count and the platelet reactivity by measuring bleeding time [61] and plasma level of vWF [55]. We observed no differences between wild-type and *EPAC1*-null mice (Fig. S4B,E). Previous *in vitro* studies reported that vWF secretion can be induced by cAMP activator forskolin [25] and EPAC-specific cAMP analogue 007-AM [25,55]. Technically, since cAMP analogues are bioactivated by esterases, there is high restriction for the applications of 007-AM *in vivo* (technical information available at http://www.biolog.de/media/TechInfo/C%20051.pdf). We applied forskolin treatment on both wild-type and observed that there is no difference in the plasma levels of vWF between wild-type and *EPAC1*-null mice (Fig. S4G).

Taken together, excessive accumulation of fibrin in the vasculatures in *EPAC1*-deficient mice is likely caused by impaired fibrinolytic activity rather than enhanced blood coagulation. These data indicate that EPAC1 may play a regulatory role in baseline fibrinolytic homeostasis.

3.2. Reduced expression of EPAC1 in endocardial tissues underneath atrial mural thrombi in humans

Hypofibrinolysis was documented in rheumatic or non-rheumatic chronic atrial fibrillation patients, and is associated with high thromboembolic risk [62,63]. EPAC actively participates in the regulation of various cAMP-dependent cardiovascular functions [35,36]. There is still a lack of information on EPAC in rheumatic heart disease. We collected endocardial tissues (including cardiac endothelium) underneath surgery-confirmed left atrial mural thrombi from four cases of rheumatic mitral stenosis with chronic atrial fibrillation. The heart endocardium is primarily made up of cardiac ECs, which are derived from vascular ECs [64]. Interestingly, WB analysis displayed that EPAC1 expression was prominently decreased, with increased levels of fibrin in the endocardial areas underneath the atrial mural thrombi compared to control tissue from normal donor hearts (Fig. 2A). IF analysis revealed enhanced fibrin(ogen) deposition compared to control tissues; fibrin (ogen) colocalized with reduced IF of EPAC1 in the endocardium and intima layer of coronary blood vessels in the cardiac wall (Fig. 2B). This suggests that there is a correlation between reduced EPAC1 and deposition of fibrin(ogen) in endothelium during formation of mural thrombi in human heart tissue.

3.3. Deletion of EPAC1 makes mice susceptible to chemical-induced carotid arterial occlusion

The ferric chloride ($FeCl_3$)-induced rodent carotid artery thrombosis model is a well-established experimental model for studying vascular fibrinolytic activity *in vivo*. In the model, the arterial occlusion caused by thrombus formation is measured by monitoring blood flow with a Doppler probe [14,65–67]. Using this model, we examined vascular fibrinolytic function in wild-type and *EPAC1*-null mice by comparing the maximal arterial occlusion (as % of baseline blood flow rate) (MaxO), maximal recovery of blood flow over 30 min after exposure to $FeCl_3$ (as % of baseline blood flow rate) (MaxR) [14], and histological observation of $FeCl_3$-induced carotid arterial thrombosis. Typical patterns of blood flow curves recorded during these experiments are illustrated (Fig. 3A). Baseline blood flow was measured first, and there was no statistical difference between wild-type and *EPAC1*-null mice (1.9556 ± 0.1078 ml/min *vs.* 1.7694 ± 0.1265 ml/min, P = 0.2748). Acute arterial thrombosis was induced by application of 7.5% $FeCl_3$ to the adventitial arterial surface of the carotid artery [14]. Compared to wild-type mice, *EPAC1*-null mice demonstrated a significantly higher MaxO (36.40 ± 4.32% *vs.* 73.55 ± 7.95%, P < 0.01) and a lower MaxR (80.44 ± 4.97% *vs.* 31.49 ± 9.01%, P < 0.01) for $FeCl_3$-exposed carotid arteries. The D-dimer assay [68] implied reduced levels of fibrin degradation observed in *EPAC1*-null mice after application of 7.5% $FeCl_3$, compared to wild-type mice after same exposure (Fig. 3C). Furthermore, in a blinded study of hematoxylin and eosin (H&E)-stained cervical tissue, thrombi were detected in 8.33% of wild-type mice; in *EPAC1*-null mice, the incidence of detected thrombi was41.67% (Table 1) (Fig. S5). These results indicate that *EPAC1*-null mice suffer more severe acute arterial occlusion caused by $FeCl_3$-induced thrombosis.

The observation that *EPAC1*-null mice are susceptible to chemical-induced carotid arterial thrombosis, coupled with evidence that decreased expression of EPAC1 in human cardiac endothelia is associated with fibrin deposition on the surface, suggests that EPAC1 plays a role in regulation of vascular accumulation of fibrin.

3.4. Reintroduction of ANXA2 attenuates chemical-induced vascular occlusion in EPAC1-null mice

We next sought to delineate the cellular and molecular mechanisms by which EPAC1 might be involved in regulation of vascular accumulation of fibrin. EPAC1 is an intracellular sensor of cAMP. In our study, *EPAC1*-null mice showed an impaired ability to resist $FeCl_3$-induced thrombosis, which is similar to the phenotypes observed in *ANXA2*-null mice [14] and *S100A10*-null mice [8]. ANXA2 and S100A10 form a complex that is the most studied tPA binding receptor expressed abundantly in ECs [7,9,11–13]. We isolated biotinylated mouse aortic endothelial surface proteins from mice and revealed decreased cell surface ANXA2 in *EPAC1*-null mice (Fig. 3E). Furthermore, recombinant ANXA2 (rANXA2) can reduce thrombus formation in the $FeCl_3$-induced rodent carotid artery thrombosis model [65]. We introduced rANXA2 intravenously (i.v.) [65] into *EPAC1*-null mice to evaluate whether vascular occlusion can be restored.

Treatment with rANXA2 or bovine serum albumin (BSA) induced no changes in baseline blood flow in either wild-type or *EPAC1*-null mice (Fig. 3A). After exposure to $FeCl_3$, there was no significant difference in either MaxO or MaxR between wild-type and *EPAC1*-null mice when they were both pretreated with rANXA2 (Fig. 3A). *EPAC1*-null mice pretreated with BSA showed decreased MaxO and increased MaxR of the $FeCl_3$-exposed carotid artery, compared to the *EPAC1*-null mice pretreated with rANXA2. Blinded histological examination revealed that thrombi were detected in 40% of *EPAC1*-null mice pretreated with BSA; in *EPAC1*-null mice pretreated with rANXA2, the incidence of detected thrombi was 9.09% (Table 1). Moreover, we isolated biotinylated mouse aortic endothelial surface proteins from rANXA2-treated mice after carotid artery exposure to $FeCl_3$ and revealed elevated level of cell surface ANXA2 in rANXA2-treated *EPAC1*-null mice, compared to BSA-treated group (Fig. 3F). These data indicate that attenuated blood flow resulting from EPAC1 depletion correlates with impaired ANXA2-mediated endothelial surface fibrinolytic activity and can be restored by intravenous administration of rANXA2.

3.5. Inactivation of EPAC1 weakens plasminogen binding to the endothelial surface and diminishes plasmin generation in an ANXA2-dependent manner

To assess the soluble part of the fibrinolytic system, we measured euglobulin clot lysis time [69] and found no differences between wild-type and *EPAC1*-null mice (Fig. S4D). We further examined levels of major components of the fibrinolytic system, including plasminogen, fibrinogen, tPA, and plasminogen activator inhibitor-1 [68], and detected no differences between wild-type and *EPAC1*-null mice (Fig. S4F). These observations suggest that the fluid-phase soluble fibrinolytic system was intact in *EPAC1*-null mice, a finding that is consistent with reduced extracellular ANXA2.

However, using a cell-based system we demonstrated that treatment of ESI09 weakened plasminogen binding to the endothelial surface and reduced plasmin generation (Fig. 3G), suggesting EPAC1 modulates plasminogen activation. In order to determine the role of ANXA2 in the regulation of EPAC1 on plasmin activation on endothelial surface, we transfected HUVECs with pEGFP-HA vectors expressing full-length ANXA2 (University of Dundee, Dundee, UK) before DMSO- or ESI09-treatment. Plasmin activity assay demonstrated that ectopic expression of ANXA2 can attenuate the inhibition of plasmin activity by inactivation of EPAC1 (Fig. 3H), suggesting that EPAC1 regulates endothelial surface plasminogen conversion in an ANXA2-dependent manner.

3.6. Inhibition of EPAC1 affects the interaction of ANXA2 with lipid rafts and impedes ANXA2 association with S100A10 in ECs

Given the fact that elevated levels of intra-endothelial cAMP can stabilize $(ANXA2\text{-}S100A10)_2$ [25], we examined the correlation among EPAC1 expression and the levels and association of ANXA2 and S100A10. First, we performed qRT-PCR and WB to measure mRNA and protein levels of ANXA2 and S100A10 in tissues from wild-type and *EPAC1*-null mice. There was no significant difference in either mRNA or protein levels between wild-type and *EPAC1*-null mice in brain, lung, and kidney tissue (Figs. S1B, S6A), suggesting that depletion of EPAC1 does not affect *de novo* protein synthesis of ANXA2 and S100A10 in these tissues.

Taking advantage of the EPAC-specific inhibitor ESI09, we determined the effect of EPAC1 inhibition on endothelial expression of ANXA2 and its partner S100A10 in the cellular membrane compartment. We treated HUVECs with ESI09 to inhibit EPAC1. Similar levels of mRNA and ANXA2 and S100A10 proteins were detected in vehicle-and ESI09-treated cells (Fig. S6B,C), indicating no correlation between pharmacological inactivation of EPAC1 and *de novo* protein synthesis of ANXA2 and S100A10. However, immunoprecipitation assays with EC samples demonstrated that ESI09 treatment reduced associated ANXA2 in S100A10 precipitates, suggesting decreased formation of $(ANXA2\text{-}S100A10)_2$ in ECs (Fig. 4A).

It has been established that ANXA2 binds to negatively charged phospholipids in cellular membranes. We therefore employed ultracentrifugation to isolate lipid rafts from membrane fraction samples of HUVECs in detergent conditions [70]. We obtained highly purified lipid rafts (Fig. S7A). In the vehicle-treated group, ANXA2 is still associated with lipid rafts after sample processing by ultracentrifugation. ESI09 treatment did not significantly affect phospholipid and cholesterol contents of lipid rafts and the total amount of lipid rafts (Fig. S7B). WB analysis revealed a significantly lower level of ANXA2 in lipid rafts in the ESI09-treated group compared to the vehicle-treated group (Fig. 4B).

These data suggest that inactivation of EPAC1 interrupts ANXA2 binding to the cell membrane and its association with S100A10.

3.7. Inhibition of EPAC1 decreases ANXA2 and S100A10 residing on EC apical surfaces

Both ANXA2 and S100A10 reside on the luminal surface of ECs mainly in the form of $(ANXA2\text{-}S100A10)_2$, a functional unit for plasmin-mediated fibrinolysis. To examine whether EPAC1 regulates the appearance of this crucial determinant for fibrinolytic activity on the EC luminal surface, we probed the expression levels of ANXA2 and S100A10 on the EC apical surface using biochemical and biomechanical approaches.

We performed impermeable cell-based ELISA assays [71,72] to probe the cell surface levels of ANXA2 and S100A10. Endothelial surface levels of ANXA2 and S100A10 were determined as relative fluorescence units corrected for cell protein (FU/A550). Comparing vehicle-, PKA-specific inhibitor H89- [33], and ESI09-treated HUVECs in 96-well plates demonstrated that EPAC inhibition significantly decreased ANXA2- ($P < 0.05$) and S100A10-specific ($P < 0.05$) signals on the surfaces of HUVECs (Fig. 5A). No difference was detected between groups of vehicle and H89. We also probed the levels of other plasminogen receptors on EC surfaces and found no differences between vehicle- and ESI09-treated HUVECs (Fig. S8).

To further validate these results, we used atomic force microscopy (AFM) to quantify the distribution of ANXA2 and S100A10 on the surface of ECs. AFM is an advanced tool for studying biomechanical properties and has been used to determine the expression levels of cell surface proteins by measuring the binding affinity of specific protein–protein interactions, including antigen–antibody and receptor–ligand, with nanoforce spectroscopy [73,74]. In our study, anti-ANXA2 or S100A10 antibodies were immobilized on polystyrene spheres attached to a colloidal cantilever. We measured the specific unbinding force during

rupture of the interaction between the antigen (ANXA2 or S100A10) expressed at the apical surface of living HUVECs and the antibody-coated AFM cantilever probe. Interactions between antibodies on the AFM cantilever and cell surface antigens cause large adhesion forces, which are quantified by the deflection signal during separation of the cantilever from the cell. By tracking the cantilever deflection and retraction cycle, the binding, stretching, and ruptures of antibody–antigen complexes can be monitored in terms of the adhesive force changes on the cantilever over the distance traveled by the cantilever. Representative force-distance (FD) curves exhibit rupture events occurring during the interaction between antigens and antibodies in designated fields on the surface of a single living HUVEC (Fig. 5B). Therefore, by integrating the areas underneath the FD curve and above the baseline (zero force in Fig. 5B), we calculated the work that is required to break all interactive bonds between the cantilever and the EC, reflecting the quantity of antigen expression on the surface [73,74]. Using an ANXA2 antibody-coated cantilever, greater unbinding work was measured on the surface of HUVECs exposed to vehicle compared with that of HUVECs exposed to ESI09 ($3.568 \pm 0.132 \times 10^4$ pN*nm vs. $1.956 \pm 0.072 \times 10^4$ pN*nm, $P < 0.01$), indicating that more ANXA2 antigens were detected on the surface of vehicle-treated HUVECs than ESI09-treated HUVECs (Fig. 5C). This suggests that EPAC1 inhibition reduces the amount of ANXA2 residing at the cell surface. Similarly, results obtained from using S100A10 antibody-coated cantilevers showed greater unbinding force on the surface of HUVECs exposed to vehicle compared to HUVECs exposed to ESI09 ($3.075 \pm 0.091 \times 10^4$ pN*nm vs$1.119 \pm 0.051 \times 10^4$ pN*nm, $P < 0.01$), suggesting more S100A10 antigens were detected on HUVEC surfaces of the vehicle-treated group than the ESI09-treated group (Fig. 5C). The presence of the blocking antibody resulted in a significant decrease in the adhesion interaction between normal cells and the functionalized cantilever. These nanobiomechanical data corroborated the evidence gained from our biochemical studies that demonstrated that EPAC1 regulates the expression of ANXA2 and S100A10 on EC apical surfaces.

3.8. Inhibition of EPAC1 decreases tyrosine 23 phosphorylation of ANXA2 (Y23phANXA2) in the cell membrane compartment

ANXA2 binding to and translocation across the cell membrane is believed to be regulated *via* posttranslational modification of ANXA2, mainly phosphorylation or dephosphorylation of the N-terminal domain [25,75]. While phosphorylation of serine 25 (S25ph) by PKC inhibits ANXA2 and S100A10 binding and externalization, phosphorylation of tyrosine 23 (Y23ph) by Src family kinases (SFK) stimulates ANXA2 binding to lipid rafts [23] and surface expressions of ANXA2 [22,23,76]. We did not observe changes in S25ph or Y23ph of ANXA2 in the post-nuclear fractions of HUVECs following ESI09 exposure (data not shown). However, ESI09 decreased Y23phANXA2 in the membrane fractions (Fig. 6A,C), implicating a role of SFK in ESI09-mediated downregulation of ANXA2 surface expression. Indeed, treatment of ESI09-exposed HUVECs with a Src family activator (SFA) [77] partially restored Y23phANXA2 in the membrane fractions and ANXA2 surface expression (Fig. 6C). These data suggest that EPAC1 regulates the dynamics of ANXA2, possibly by modulating Src kinase family-mediated phosphorylation of the N-terminal domain of ANXA2.

4. Discussion

Interrupted blood flow caused by a thrombus is the pathological foundation of some major human diseases. Fibrin, which is the main structural scaffold of a blood clot, is the ultimate product of coagulation and the major target of fibrinolysis [78]. Excessive accumulation of fibrin in tissue can be caused by enhanced blood coagulation or insufficiency in fibrinolytic function [8]. We detected increased fibrin accumulation in the microvasculature of multiple organs and decreased level of endothelial surface ANXA2 in *EPAC1*-null mice compared with wild-type mice, while there were no differences in measurements of coagulation. Inactivation of EPAC1 inhibits binding of plasminogen to the EC surface and its activation and ectopic expression of ANXA2 can mitigate this inhibitory effect and improve the plasmin generation. Reintroduction of ANXA2 ameliorates endothelial surface level of ANXA2 and attenuates chemical-induced vascular occlusion in *EPAC1*-null mice. This observation suggests that the increased fibrin accumulation detected in *EPAC1*-null mice is likely the result of impaired fibrinolysis rather than enhanced blood coagulation.

Plasmin is the key protease involved in the dissolution of a fibrin clot. Among identified endothelial surface plasminogen and PA binding receptors, the $(ANXA2\text{-}S100A10)_2$ has been potentially linked to the cAMP-EPAC signaling axis. In the context of coagulation-relevant regulation in HUVECs, the formation and stabilization of $(ANXA2\text{-}S100A10)_2$ occurs in a cAMP-dependent manner [25]. The cAMP-EPAC pathway has been studied in cellular biological activities such as cell adhesion, cell junction, cell secretion, and cell differentiation [32,37]. In ECs, EPAC1 and not EPAC2 is the dominant functional isoform [1,43,53]. EPAC1 is responsible for endothelial microtubule dynamics, cell secretion, angiogenesis, and barrier functions [1,25,40,47,79]. In the present study, our *EPAC1*-null mice displayed excessive fibrin accumulation in the microvasculature of multiple organs. Compared with wild-type mice, *EPAC1*-null mice showed an inability to resist acute arterial occlusion caused by $FeCl_3$-induced thrombosis. *In vitro* studies revealed that inactivation of EPAC1 weakens plasminogen binding to the EC surface and diminishes plasmin generation. These results suggest that EPAC1 deficiency impaired fibrinolytic function. Our study, for the first time, showed the possible role of EPAC1 in regulating EC fibrinolysis.

Interestingly, *ANXA2*-null mice [14] and *S100A10*-null mice [8] both also exhibited impaired fibrinolytic function, strongly suggesting that EPAC1 and $(ANXA2\text{-}S100A10)_2$ may act cooperatively to mediate the fibrinolytic pathway. Employing biochemical and biomechanical technologies, we have obtained the following new lines of evidence: (1) inactivation of EPAC1 downregulated the level of associated ANXA2 in S100A10 precipitates in ECs; (2) inactivation of EPAC1 decreased ANXA2 and S100A10 expression in ECs at the apical surface; and (3) AFM experiments revealed a dramatic reduction in the interactive forces between ANXA2- or S100A10-functionalized cantilevers and endothelial surfaces after inhibition of EPAC1 in ECs.

Taken together, these data reveal a tight association between EPAC1 and the dynamics of $(ANXA2\text{-}S100A10)_2$ in ECs. $(ANXA2\text{-}S100A10)_2$, which is expressed on both resting and activated ECs, possesses binding affinity for both plasminogen and tPA and serves as receptor for tPA-dependent plasmin generation on endothelial luminal surfaces [9,11–13].

Regulation of this heterotetramer, either by formation, stabilization, or translocation, modulates fibrinolytic activity on the EC luminal surface. We probed the downregulated level of EC surface ANXA2 in *EPAC1*-null mice. The fact that *EPAC1*-null mice given rANXA2 intravenously restored the aortic vascular luminal surface level of ANXA2 after carotid artery exposure to $FeCl_3$ and gained the capability to attenuate acute arterial occlusion in a chemically-induced thrombosis model further supports our interpretation that EPAC1 plays a critical role in $(ANXA2\text{-}S100A10)_2$-mediated vascular fibrinolysis. Furthermore, we observed that ectopic expression of ANXA2 can partially ameliorate ESI09 treatment-induced decreased plasmin generation on EC surface, suggesting that EPAC1 regulated vascular endothelial surface plasminogen activation in a ANXA2-dependent manner.

Despite our evidence supporting a connection between EPAC1 and $(ANXA2\text{-}S100A10)_2$-mediated fibrinolysis, the underlying mechanism remains unclear. Translocation of $(ANXA2\text{-}S100A10)_2$ occurs independently of the classical endoplasmic reticulum–Golgi pathway and does not involve *de novo* protein synthesis [11,22,80]. The S100A10-binding motif is found in the N-terminal domain of ANXA2 [12,81]. ANXA2 lacks a typical signal peptide [22]. ANXA2 in the cellular membrane compartment is believed to be regulated mainly *via* phosphorylation/dephosphorylation of the N-terminal domain of ANXA2 [25,75], which is catalyzed by serine/threonine kinases, serine/threonine phosphatase, or tyrosine kinase [22,25,75]. Three phosphorylation sites (serine 11, tyrosine 23, and serine 25) have been identified as being functionally relevant to the regulation of ANXA2 [82]. Brandherm et al. [25] identified that serine 11 dephosphorylation in ANXA2, catalyzed by a calcineurin-like phosphatase, is a positive switch for cAMP-dependent extracellular trafficking of $(ANXA2\text{-}S100A10)_2$. Furthermore, He et al. reported that protein kinase C-activated phosphorylation of ANXA2 at serines 11 and 25 resulted in disassociation of $(ANXA2\text{-}S100A10)_2$ and prevented ANXA2's translocation to the cell surface [75]. However, phosphorylation of serine 11 has only been investigated *in vitro* [82]. Phosphorylation of serine 11 works as a regulator on the translocation of ANXA2 and cAMP-PKA-regulated vWF secretion [25]. Our study demonstrates that inactivation of EPAC1 down-regulates the phosphorylation of tyrosine 23 of ANXA2, another phosphorylation site identified functionally relevant to the regulation of ANXA2 translocation, and does not impact on the constitutional level of vWF in the plasma and other major hematological parameters. Y23phANXA2 was identified as another regulatory switch during association of ANXA2 with lipid rafts [23] and translocation of $(ANXA2\text{-}S100A10)_2$ [22]. After Y23phANXA2 through Src family tyrosine kinase (s)-dependent pathway, the heterotetramer is translocated to the cell surface by an as yet unknown mechanism [22,23,76]. In this study we have shown that inactivation of EPAC1 by ESI09 decreased Y23phANXA2 in the EC membrane compartment, which might be responsible for the reduced ANXA2 surface expression. Importantly, this defect could be partially restored by treating cells with a SFA, suggesting a positive regulatory role for EPAC1 in SFK activation. Manipulating SFK may have potential therapeutic benefits for patients with EPAC1 deficiency [83]. Additional work is needed to elucidate the precise mechanism by which EPAC1 regulates ANXA2 phosphorylation and surface translocation. EPAC proteins exert regulatory effects in a complex downstream signaling scheme by coupling a multitude of

effectors. The precise mechanisms by which Epac1 regulates Src kinase family-mediated ANXA2 phosphorylation to govern ANXA2 translocation in the context of vascular fibrinolytic function remain unknown. This represents a major challenge during our ongoing and future investigations.

In contrast to our study, Yang et al. recently reported that EPAC1 inhibition increases ANXA2 surface expression in HUVECs [84]. This discrepancy could be due to the different reagents and experimental conditions used in the *in vitro* experiments (*i.e.* applications of cAMP and EPAC activator, assay protocols, and the ways samples were collected). While in our study we used ESI09 to treat cells for 24 h, an EPAC-specific cAMP analog 007-AM was used in the presence or absence of another ESI HJC0758 to treat cells for 30 min in Yang's study. Given that 007-AM has been reported to promote exocytosis of WPBs and increase secretion of vWF [55], these potential effects, which were not examined in that study, could confound the observed results related to fibrinolysis. Second, when assessing plasminogen activation it is imperative to thoroughly wash the HUVECs prior to incubation with the assay medium [85,86] to avoid direct/indirect effects of ESI or EPAC activators on the measuring. This critical washing step is not evident in Yang's study. To our knowledge, there is no published method to directly measure plasminogen activation in culture medium [85–87]. Third, since ANXA2 is dominantly detected in cytosol and nuclear areas [16,21], we isolated membrane fractions to measure the translocation of ANXA2 across plasma membrane. However, whole cell lyses were used in Yang's study. Last but not least, Yang et al. used EGTA to collect surface proteins from HJC0785-treated HUVECs. In our hand, even a brief treatment of EDTA caused ESI09-treated HUVEVs detach after edge curling up, thus it was not possible for us to use this method to isolate apical membrane proteins. Instead, we used AFM to directly measure ANXN2 protein levels at the apical surface of HUVECs.

In conclusion, our studies combined an *in vitro* primary human endothelial system with an *in vivo* model and linked EPAC1 with the $(ANXA2\text{-}S100A10)_2$-based fibrinolytic pathway to reveal a novel role for EPAC1 in vascular fibrinolysis. In ECs, EPAC1 is responsible for the formation and translocation of $(ANXA2\text{-}S100A10)_2$, a key endothelial surface platform for tPA and plasminogen, aiding the conversion of plasminogen to plasmin.

Supplementary Material

Refer to Web version on PubMed Central for supplementary material.

Acknowledgements

We gratefully acknowledge Dr. Edward Nelson for his important contributions for establishing the capacity of the atomic force microscopy (AFM) system, data analysis, and critical review of the manuscript. We gratefully acknowledge Drs. David Walker and Kimberly Schuenke for their critical reviews and editing of the manuscript. We thank Drs. Katherine Hajjar, Vladimir Motin, Vsevolod Popov, and Paul Boor for input during the planning phases of the experiments. We thank Xiang Li for assistance during revision. This work was supported by NIH grant R01 AI121012 (B.G.), National Natural Science Foundation of China grant 81370265 (F.L.), and NIH grants R01NS079166 and R01NS095747 (S.J.T.). The funders had no role in the study design, data collection and analysis, decision to publish, or preparation of the manuscript.

References

[1]. Kooistra MR, Corada M, Dejana E, Bos JL, Epac1 regulates integrity of endothelial cell junctions through VE-cadherin, FEBS Lett. 579 (22) (2005) 4966–4972. [PubMed: 16115630]

[2]. Dejana E, Giampietro C, Vascular endothelial-cadherin and vascular stability, Curr. Opin. Hematol 19 (3) (2012) 218–223. [PubMed: 22395663]

[3]. Wang S, Aurora AB, Johnson BA, et al., The endothelial-specific microRNA miR-126 governs vascular integrity and angiogenesis, Dev. Cell 15 (2) (2008) 261–271. [PubMed: 18694565]

[4]. Chapin JC, Hajjar KA, Fibrinolysis and the control of blood coagulation, Blood Rev. 29 (2015) 17–24. [PubMed: 25294122]

[5]. Madoiwa S, Recent advances in disseminated intravascular coagulation: endothelial cells and fibrinolysis in sepsis-induced DIC, J. Intensive Care 3 (2015) 8. [PubMed: 27408725]

[6]. Urano T, Suzuki Y, Accelerated fibrinolysis and its propagation on vascular endothelial cells by secreted and retained tPA, J Biomed Biotechnol 2012 (2012) 208108. [PubMed: 23118500]

[7]. Godier A, Hunt BJ, Plasminogen receptors and their role in the pathogenesis of inflammatory, autoimmune and malignant disease, J. Thromb. Haemost 11 (1) (2013) 26–34. [PubMed: 23140188]

[8]. Surette AP, Madureira PA, Phipps KD, Miller VA, Svenningsson P,Waisman DM, Regulation of fibrinolysis by S100A10 in vivo, Blood 118 (11) (2011) 3172–3181. [PubMed: 21768297]

[9]. Dassah M, Deora AB, He K, Hajjar KA, The endothelial cell annexin A2 system and vascular fibrinolysis, Gen. Physiol. Biophys 28 (2009) F20–F28 (Spec No Focus). [PubMed: 20093722]

[10]. Cesarman-Maus G, Hajjar KA, Molecular mechanisms of fibrinolysis, Br. J. Haematol 129 (3) (2005) 307–321. [PubMed: 15842654]

[11]. Liu Y, Myrvang HK, Dekker LV, Annexin A2 complexes with S100 proteins: structure, function and pharmacological manipulation, Br. J. Pharmacol 172 (2015) 1664–1676. [PubMed: 25303710]

[12]. Bharadwaj A, Bydoun M, Holloway R, Waisman D, Annexin A2 heterotetramer: structure and function, Int. J. Mol. Sci 14 (3) (2013) 6259–6305. [PubMed: 23519104]

[13]. Das R, Burke T, Plow EF, Histone H2B as a functionally important plasminogen receptor on macrophages, Blood 110 (10) (2007) 3763–3772. [PubMed: 17690254]

[14]. Ling Q, Jacovina AT, Deora A, et al., Annexin II regulates fibrin homeostasis and neoangiogenesis in vivo, J. Clin. Invest 113 (1) (2004) 38–48. [PubMed: 14702107]

[15]. Hajjar KA, Jacovina AT, Chacko J, An endothelial cell receptor for plasminogen/tissue plasminogen activator. I. Identity with annexin II, J. Biol. Chem 269 (33) (1994) 21191–21197. [PubMed: 8063740]

[16]. Luo M, Hajjar KA, Annexin A2 system in human biology: cell surface and beyond, Semin. Thromb. Hemost 39 (4) (2013) 338–346. [PubMed: 23483454]

[17]. He KL, Deora AB, Xiong H, et al., Endothelial cell annexin A2 regulates polyubiquitination and degradation of its binding partner S100A10/p11, J. Biol. Chem 283 (28) (2008) 19192–19200. [PubMed: 18434302]

[18]. Nazmi AR, Ozorowski G, Pejic M, Whitelegge JP, Gerke V, Luecke H, N-terminal acetylation of annexin A2 is required for S100A10 binding, Biol. Chem 393 (10) (2012) 1141–1150. [PubMed: 23091277]

[19]. Menke M, Gerke V, Steinem C, Phosphatidylserine membrane domain clustering induced by annexin A2/S100A10 heterotetramer, Biochemistry 44 (46) (2005) 15296–15303. [PubMed: 16285733]

[20]. Morel E, Gruenberg J, Annexin A2 binding to endosomes and functions in endosomal transport are regulated by tyrosine 23 phosphorylation, J. Biol. Chem 284(3) (2009) 1604–1611. [PubMed: 18990701]

[21]. Hajjar KA, The biology of annexin A2: from vascular fibrinolysis to innate immunity, Trans. Am. Clin. Climatol. Assoc 126 (2015) 144–155. [PubMed: 26330668]

[22]. Deora AB, Kreitzer G, Jacovina AT, Hajjar KA, An annexin 2 phosphorylation switch mediates p11-dependent translocation of annexin 2 to the cell surface, J. Biol. Chem 279 (42) (2004) 43411–43418. [PubMed: 15302870]

[23]. Valapala M, Vishwanatha JK, Lipid raft endocytosis and exosomal transport facilitate extracellular trafficking of annexin A2, J. Biol. Chem 286 (35) (2011) 30911–30925. [PubMed: 21737841]

[24]. Hubaishy I, Jones PG, Bjorge J, et al., Modulation of annexin II tetramer by tyrosine phosphorylation, Biochemistry 34 (44) (1995) 14527–14534. [PubMed: 7578058]

[25]. Brandherm I, Disse J, Zeuschner D, Gerke V, cAMP-induced secretion of endothelial von Willebrand factor is regulated by a phosphorylation/dephosphorylation switch in annexin A2, Blood 122 (6) (2013) 1042–1051. [PubMed: 23757730]

[26]. Beavo JA, Brunton LL, Cyclic nucleotide research — still expanding after half a century, Nat. Rev. Mol. Cell Biol 3 (9) (2002) 710–718. [PubMed: 12209131]

[27]. Lefkimmiatis K, Zaccolo M, cAMP signaling in subcellular compartments, Pharmacol. Ther 143 (3) (2014) 295–304. [PubMed: 24704321]

[28]. Gold MG, Gonen T, Scott JD, Local cAMP signaling in disease at a glance, J. Cell Sci 126 (Pt 20) (2013) 4537–4543. [PubMed: 24124191]

[29]. Di Benedetto G, Pendin D, Greotti E, Pizzo P, Pozzan T, Ca2+ and cAMP cros-stalk in mitochondria, J. Physiol 592 (2) (2014) 305–312. [PubMed: 23858012]

[30]. Hofer AM, Interactions between calcium and cAMP signaling, Curr. Med. Chem 19 (34) (2012) 5768–5773. [PubMed: 22963560]

[31]. Borland G, Smith BO, Yarwood SJ, EPAC proteins transduce diverse cellular actions of cAMP, Br. J. Pharmacol 158 (1) (2009) 70–86. [PubMed: 19210747]

[32]. Cheng X, Ji Z, Tsalkova T, Mei F, Epac and PKA: a tale of two intracellular cAMP receptors, Acta Biochim. Biophys. Sin. Shanghai 40 (7) (2008) 651–662. [PubMed: 18604457]

[33]. de Rooij J, Zwartkruis FJ, Verheijen MH, et al., Epac is a Rap1 guanine-nucleotide-exchange factor directly activated by cyclic AMP, Nature 396 (6710) (1998) 474–477. [PubMed: 9853756]

[34]. Kawasaki H, Springett GM, Mochizuki N, et al., A family of cAMP-binding proteins that directly activate Rap1, Science 282 (5397) (1998) 2275–2279. [PubMed: 9856955]

[35]. Lezoualc'h F, Fazal L, Laudette M, Conte C, Cyclic AMP sensor EPAC proteins and their role in cardiovascular function and disease, Circ. Res 118 (5) (2016) 881–897. [PubMed: 26941424]

[36]. Métrich M, Berthouze M, Morel E, Crozatier B, Gomez AM, Lezoualc'h F, Role of the cAMP-binding protein Epac in cardiovascular physiology and pathophysiology, Pflugers Arch. 459 (4) (2010) 535–546. [PubMed: 19855995]

[37]. Gloerich M, Bos JL, Epac: defining a new mechanism for cAMP action, Annu. Rev. Pharmacol. Toxicol 50 (2010) 355–375. [PubMed: 20055708]

[38]. Milne GR, Palmer TM, Yarwood SJ, Novel control of cAMP-regulated transcription in vascular endothelial cells, Biochem. Soc. Trans 40 (1) (2012) 1–5. [PubMed: 22260656]

[39]. Pannekoek WJ, van Dijk JJ, Chan OY, et al., Epac1 and PDZ-GEF cooperate in Rap1 mediated endothelial junction control, Cell. Signal 23 (12) (2011) 2056–2064. [PubMed: 21840392]

[40]. Sehrawat S, Cullere X, Patel S, Italiano J, Mayadas TN, Role of Epac1, an exchange factor for Rap GTPases, in endothelial microtubule dynamics and barrier function, Mol. Biol. Cell 19 (3) (2008) 1261–1270. [PubMed: 18172027]

[41]. Noda K, Zhang J, Fukuhara S, Kunimoto S, Yoshimura M, Mochizuki N, Vascular endothelial-cadherin stabilizes at cell-cell junctions by anchoring to circumferential actin bundles through alpha- and beta-catenins in cyclic AMP-Epac-Rap1 signal-activated endothelial cells, Mol. Biol. Cell 21 (4) (2010) 584–596. [PubMed: 20032304]

[42]. Parnell E, Yarwood SJ, Interactions between Epac1 and ezrin in the control of endothelial barrier function, Biochem. Soc. Trans 42 (2) (2014) 274–278. [PubMed: 24646230]

[43]. Cullere X, Shaw SK, Andersson L, Hirahashi J, Luscinskas FW, Mayadas TN, Regulation of vascular endothelial barrier function by Epac, a cAMP-activated exchange factor for Rap GTPase, Blood 105 (5) (2005) 1950–1955. [PubMed: 15374886]

[44]. Sands WA, Woolson HD, Milne GR, Rutherford C, Palmer TM, Exchange protein activated by cyclic AMP (Epac)-mediated induction of suppressor of cytokine signaling 3 (SOCS-3) in vascular endothelial cells, Mol. Cell. Biol 26 (17) (2006) 6333–6346. [PubMed: 16914720]

[45]. Wiejak J, Dunlop J, Yarwood SJ, The role of c-Jun in controlling the EPAC1-dependent induction of the SOCS3 gene in HUVECs, FEBS Lett. 588 (9) (2014) 1556–1561. [PubMed: 24631457]

[46]. Lehrke M, Kahles F, Makowska A, et al., PDE4 inhibition reduces neointima formation and inhibits VCAM-1 expression and histone methylation in an Epac-dependent manner, J. Mol. Cell. Cardiol 81 (2015) 23–33. [PubMed: 25640159]

[47]. Doebele RC, Schulze-Hoepfner FT, Hong J, et al., A novel interplay between Epac/Rap1 and mitogen-activated protein kinase kinase 5/extracellular signal-regulated kinase 5 (MEK5/ERK5) regulates thrombospondin to control angiogenesis, Blood 114 (20) (2009) 4592–4600. [PubMed: 19710505]

[48]. Namkoong S, Kim CK, Cho YL, et al., Forskolin increases angiogenesis through the coordinated cross-talk of PKA-dependent VEGF expression and Epac-mediated PI3K/Akt/eNOS signaling, Cell. Signal 21 (6) (2009) 906–915. [PubMed: 19385062]

[49]. Shimonaka M, Katagiri K, Nakayama T, et al., Rap1 translates chemokine signals to integrin activation, cell polarization, and motility across vascular endothelium under flow, J. Cell Biol 161 (2) (2003) 417–427. [PubMed: 12707305]

[50]. Lorenowicz MJ, van Gils J, de Boer M, Hordijk PL, Fernandez-Borja M, Epac1-Rap1 signaling regulates monocyte adhesion and chemotaxis, J. Leukoc. Biol 80 (6) (2006) 1542–1552. [PubMed: 16940330]

[51]. Wittchen ES, Worthylake RA, Kelly P, Casey PJ, Quilliam LA, Burridge K, Rap1 GTPase inhibits leukocyte transmigration by promoting endothelial barrier function, J. Biol. Chem 280 (12) (2005) 11675–11682. [PubMed: 15661741]

[52]. Gong B, Shelite T, Mei FC, et al., Exchange protein directly activated by cAMP plays a critical role in bacterial invasion during fatal rickettsioses, Proc. Natl. Acad. Sci. U. S. A 110 (48) (2013) 19615–19620. [PubMed: 24218580]

[53]. Fukuhara S, Sakurai A, Sano H, et al., Cyclic AMP potentiates vascular endothelial cadherin-mediated cell-cell contact to enhance endothelial barrier function through an Epac-Rap1 signaling pathway, Mol. Cell. Biol 25 (1) (2005) 136–146. [PubMed: 15601837]

[54]. Hegeman RJ, van den Eijnden-Schrauwen Y, Emeis JJ, Adenosine 3′:5′-cyclic monophosphate induces regulated secretion of tissue-type plasminogen activator and von Willebrand factor from cultured human endothelial cells, Thromb. Haemost 79 (4) (1998) 853–858. [PubMed: 9569204]

[55]. van Hooren KW, van Agtmaal EL, Fernandez-Borja M, van Mourik JA,Voorberg J, Bierings R, The Epac-Rap1 signaling pathway controls cAMP-mediated exocytosis of Weibel-Palade bodies in endothelial cells, J. Biol. Chem 287 (29) (2012) 24713–24720. [PubMed: 22511766]

[56]. Tsalkova T, Mei FC, Li S, et al., Isoform-specific antagonists of exchange proteins directly activated by cAMP, Proc. Natl. Acad. Sci. U. S. A 109 (45) (2012) 18613–18618. [PubMed: 23091014]

[57]. Almahariq M, Chao C, Mei FC, et al., Pharmacological inhibition and genetic knockdown of exchange protein directly activated by cAMP 1 reduce pancreatic cancer metastasis in vivo, Mol. Pharmacol 87 (2) (2015) 142–149. [PubMed: 25385424]

[58]. Gong B, Lee YS, Lee I, et al., Compartmentalized, functional role of angiogenin during spotted fever group rickettsia-induced endothelial barrier dysfunction: evidence of possible mediation by host tRNA-derived small noncoding RNAs, BMC Infect. Dis 13 (2013) 285. [PubMed: 23800282]

[59]. Kopperud RK, Rygh CB, Karlsen TV, et al., Increased microvascular permeability in mice lacking Epac1 (Rapgef3), Acta Physiol (Oxford) 219 (2) (2017) 441–452.

[60]. Yan J, Mei FC, Cheng H, et al., Enhanced leptin sensitivity, reduced adiposity, and improved glucose homeostasis in mice lacking exchange protein directly activated by cyclic AMP isoform 1, Mol. Cell. Biol 33 (5) (2013) 918–926. [PubMed: 23263987]

[61]. Jirouskova M, Shet AS, Johnson GJ, A guide to murine platelet structure, function, assays, and genetic alterations, J. Thromb. Haemost 5 (4) (2007) 661–669. [PubMed: 17403200]

[62]. Atalar E, Ozmen F, Haznedaroglu I, et al., Impaired fibrinolytic capacity in rheumatic mitral stenosis with or without atrial fibrillation and nonrheumatic atrial fibrillation, Int. J. Hematol 76 (2) (2002) 192–195. [PubMed: 12215020]

[63]. Murugesan V, Pulimamidi VK, Rajappa M, Satheesh S, Revathy G,Harichandrakumari KT, Elevated fibrinogen and lowered homocysteine-vitamin determinants and their association with left atrial thrombus in patients with rheumatic mitral stenosis, Br. J. Biomed. Sci 72 (3) (2015) 102–106.

[64]. Milgrom-Hoffman M, Harrelson Z, Ferrara N, Zelzer E, Evans SM, Tzahor E, The heart endocardium is derived from vascular endothelial progenitors, Development 138 (21) (2011) 4777–4787. [PubMed: 21989917]

[65]. Ishii H, Yoshida M, Hiraoka M, et al., Recombinant annexin II modulates impaired fibrinolytic activity in vitro and in rat carotid artery, Circ. Res 89 (12) (2001) 1240–1245. [PubMed: 11739291]

[66]. Konstantinides S, Schäfer K, Thinnes T, Loskutoff DJ, Plasminogen activator inhibitor-1 and its cofactor vitronectin stabilize arterial thrombi after vascular injury in mice, Circulation 103 (4) (2001) 576–583. [PubMed: 11157725]

[67]. Li W, McIntyre TM, Silverstein RL, Ferric chloride-induced murine carotid arterial injury: a model of redox pathology, Redox Biol. 1 (2013) 50–55. [PubMed: 25101237]

[68]. Hijazi N, Abu Fanne R, Abramovitch R, et al., Endogenous plasminogen activators mediate progressive intracerebral hemorrhage after traumatic brain injury in mice, Blood 125 (16) (2015) 2558–2567. [PubMed: 25673638]

[69]. Smith AA, Jacobson LJ, Miller BI, Hathaway WE, Manco-Johnson MJ, A new euglobulin clot lysis assay for global fibrinolysis, Thromb. Res 112 (5–6) (2003) 329–337. [PubMed: 15041279]

[70]. Abbal C, Lambelet M, Bertaggia D, et al., Lipid raft adhesion receptors and Syk regulate selectin-dependent rolling under flow conditions, Blood 108 (10) (2006) 3352–3359. [PubMed: 16849645]

[71]. Wolff B, Zsak M, Rabeck C, Immunofluorescence assay for the quantitative and qualitative evaluation of intracellular interleukin-8 in microtiter plates, Anal. Biochem 244 (1) (1997) 33–39. [PubMed: 9025904]

[72]. Friis T, Kjaer Sørensen B, Engel AM, Rygaard J, Houen G, A quantitative ELISA-based co-culture angiogenesis and cell proliferation assay, APMIS 111 (6) (2003) 658–668. [PubMed: 12969022]

[73]. Mostowy S, Janel S, Forestier C, et al., A role for septins in the interaction between the listeria monocytogenes INVASION PROTEIN InlB and the Met receptor, Biophys. J 100 (8) (2011) 1949–1959. [PubMed: 21504731]

[74]. Gong B, Ma L, Liu Y, et al., Rickettsiae induce microvascular hyperpermeability via phosphorylation of VE-cadherins: evidence from atomic force microscopy and biochemical studies, PLoS Negl. Trop. Dis 6 (6) (2012) e1699. [PubMed: 22720111]

[75]. He KL, Sui G, Xiong H, et al., Feedback regulation of endothelial cell surface plasmin generation by PKC-dependent phosphorylation of annexin A2, J. Biol. Chem 286 (17) (2011) 15428–15439. [PubMed: 21115493]

[76]. Matsuda D, Nakayama Y, Horimoto S, et al., Involvement of Golgi-associated Lyn tyrosine kinase in the translocation of annexin II to the endoplasmic reticulum under oxidative stress, Exp. Cell Res 312 (7) (2006) 1205–1217. [PubMed: 16527271]

[77]. Park SY, Yang JS, Schmider AB, Soberman RJ, Hsu VW, Coordinated regulation of bidirectional COPI transport at the Golgi by CDC42, Nature 521 (7553) (2015) 529–532. [PubMed: 25945738]

[78]. Mosesson MW, Fibrinogen and fibrin structure and functions, J. Thromb. Haemost 3 (8) (2005) 1894–1904. [PubMed: 16102057]

[79]. Parnell E, Smith BO, Palmer TM, Terrin A, Zaccolo M, Yarwood SJ, Regulation of the inflammatory response of vascular endothelial cells by EPAC1, Br. J. Pharmacol 166 (2) (2012) 434–446. [PubMed: 22145651]

[80]. Gerke V, Moss SE, Annexins: from structure to function, Physiol. Rev 82 (2) (2002) 331–371. [PubMed: 11917092]

[81]. Hajjar KA, Mauri L, Jacovina AT, et al., Tissue plasminogen activator binding to the annexin II tail domain. Direct modulation by homocysteine, J. Biol. Chem 273(16) (1998) 9987–9993. [PubMed: 9545344]

[82]. Grindheim AK, Saraste J, Vedeler A, Protein phosphorylation and its role in the regulation of annexin A2 function, Biochim. Biophys. Acta 1861 (11 Pt A) (2017) 2515–2529.

[83]. Schmidt M, Dekker FJ, Maarsingh H, Exchange protein directly activated by cAMP (epac): a multidomain cAMP mediator in the regulation of diverse biological functions, Pharmacol. Rev 65 (2) (2013) 670–709. [PubMed: 23447132]

[84]. Yang W, Mei FC, Cheng X, EPAC1 regulates endothelial annexin A2 cell surface translocation and plasminogen activation, FASEB J 32 (4) (2018) 2212–2222. [PubMed: 29217666]

[85]. Ellis V, Whawell SA, Vascular smooth muscle cells potentiate plasmin generation by both urokinase and tissue plasminogen activator-dependent mechanisms: evidence for a specific tissue-type plasminogen activator receptor on these cells, Blood 90 (6) (1997) 2312–2322. [PubMed: 9310482]

[86]. O'Connell PA, Surette AP, Liwski RS, Svenningsson P, Waisman DM, S100A10 regulates plasminogen-dependent macrophage invasion, Blood 116 (7) (2010) 1136–1146. [PubMed: 20424186]

[87]. Welling TH, Huber TS, Messina LM, Stanley JC, Tissue plasminogen activator increases canine endothelial cell proliferation rate through a plasmin-independent, receptor-mediated mechanism, J. Surg. Res 66 (1) (1996) 36–42. [PubMed: 8954829]

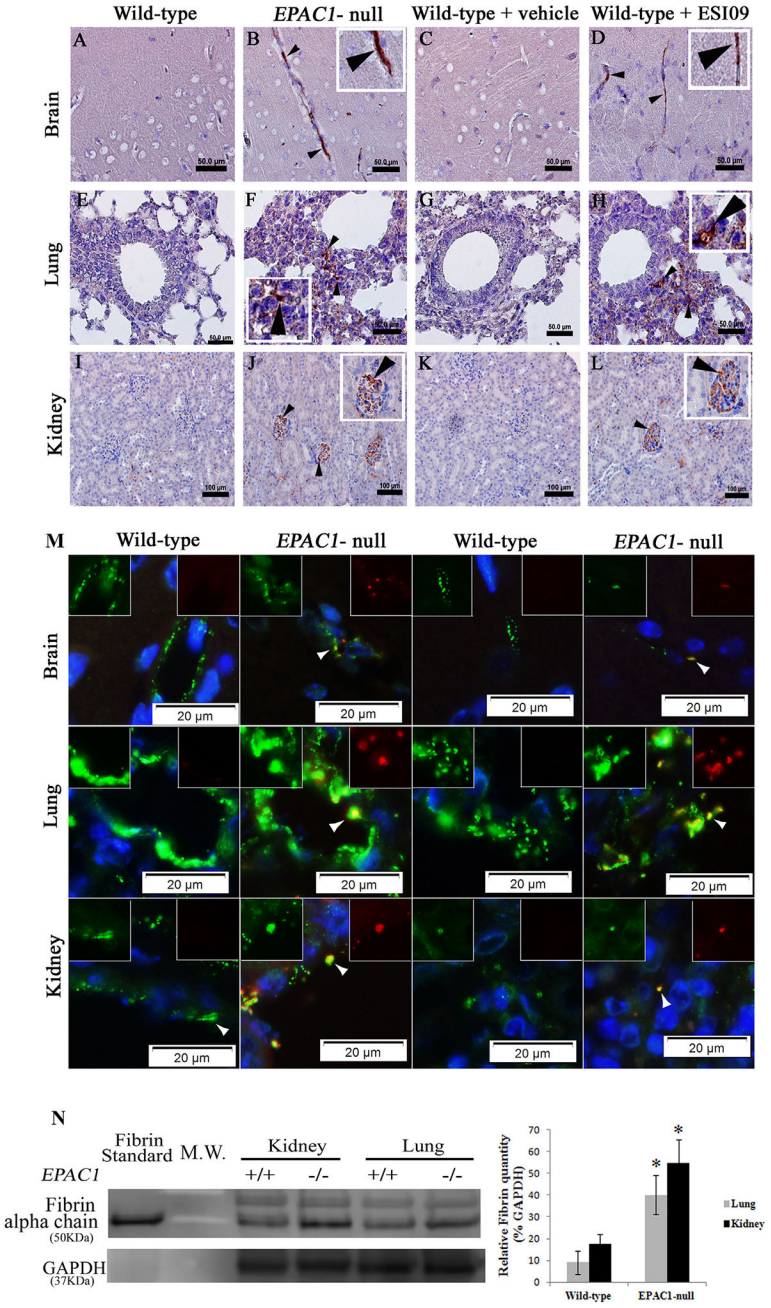

Fig. 1.

Absence of EPAC1 gene or pharmacological inactivation of EPAC1 results in fibrin deposition in microvasculature in mice. Representative immunohistochemical (IHC) analysis of brain (A–D), lung (E–H), and kidney (I–L) tissues collected from wild-type and *EPAC1*-null mice, as well as wild-type mice treated intraperitoneally with ESI09 or vehicle only after extensive perfusion *in vivo*, is shown. Arrowheads indicate fibrin(ogen) deposition in brain, lung, and renal blood vessels in both *EPAC1*-null and ESI09-treated wild-type mice. Scale bars indicate 50 μm (A-H) or 100 μm (I-L). Colocalizations (arrowheads) of fibrin(ogen) (red) with von Willebrand factor (vWF) (green) are visualized by dual-target

immunofluorescent (IF) staining (M). Normal rabbit serum was used as an antibody control in IHC and IF (Fig. S3). Western immunoblotting (WB) and densitometry analyses (M) of fibrin in mouse tissues from wild-type (n = 4) and *EPAC1*-null (n = 4) mice were normalized using GAPDH-specific controls. Standard: human fibrin protein (Sigma-Aldrich). *P < 0.05 compared with wild-type group.

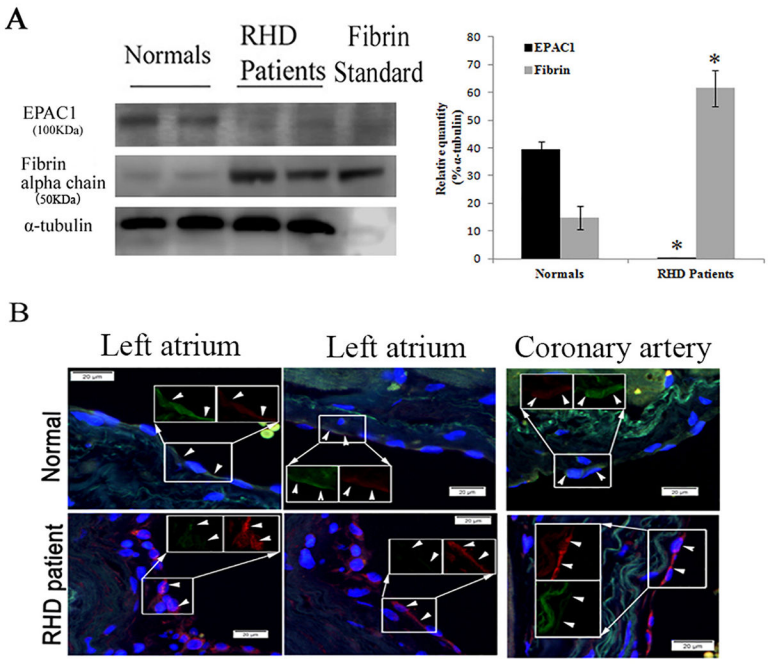

Fig. 2.

Reduced expression of EPAC1 and increased expression of fibrin in endocardial tissues underneath atrial mural thrombi in humans. Representative WB (A) shows markedly reduced expression of EPAC1 and increased expression of fibrin in endocardial areas (including cardiac endothelium) underneath atrial mural thrombi from patients with rheumatic heart disease (RHD) mitral stenosis with chronic atrial fibrillation compared to normal donor heart cases. Densitometry was used to quantify the relative intensity of EPAC1- and fibrin-specific immunoblots from patients (n = 4) and normal cases (n = 4) normalized by α-tubulin-specific controls. EPAC1 levels are presented as percentages of the indicated loading controls (*P < 0.01, compared to normal control). Representative dual-target IF staining localizes EPAC1 (green) and fibrin(ogen) (red) in areas (arrowheads) of right atrial endocardium and intima layer of coronary blood vessel walls (B). Inserts depict split signals of EPAC1 (green) and fibrin(ogen) (red) from the same area. Standard: human fibrin protein (Sigma-Aldrich). Scale bars indicate 20 μm.

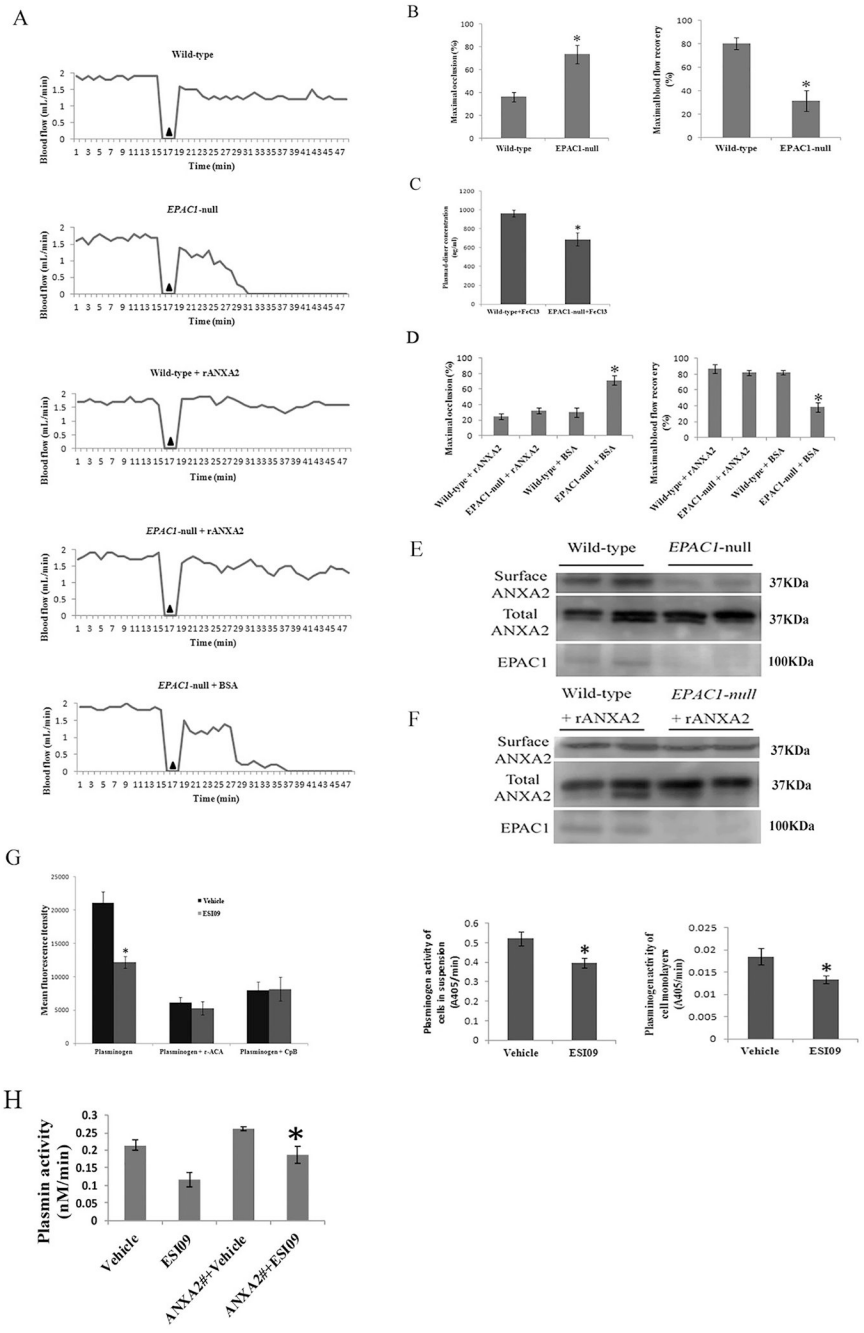

Fig. 3.

Impaired vascular fibrinolytic function can be restored by recombinant ANXA2 in *EPAC1*-null mice. Representative carotid blood flow before and after three-minute application of 7.5% $FeCl_3$ (▲) (A). Compared to wild-type mice (n = 12), *EPAC1*-null mice (n = 12) demonstrated a significantly higher maximal occlusion (MaxO, *P < 0.01) and a lower maximal recovery (MaxR, *P < 0.01) (B). Plasma levels of D-dimer were measured after application of 7.5% $FeCl_3$ (C). Compared to wild-type mice (n = 5), *EPAC1-null* mice (n = 5) demonstrated lower levels of D-dimer (*P < 0.05). Wild-type (n = 4) and *EPAC1-null* mice (n = 11) were treated with rANXA2, showing no difference in MaxO and MaxR.

Compared to *EPAC1*-null mice pretreated with BSA (n = 5), *EPAC1*-null mice pretreated with rANXA2 show lower MaxO (*P < 0.01) and higher MaxR (*P < 0.01) (D). WB analysis showed that reduced cell surface expression of ANXA2 in *EPAC1*-null mice *in vivo* (E). WB analysis further showed elevated level of aortic endothelial surface ANXA2 in rANXA2-treated *EPAC1*-null mice after carotid artery exposure to $FeCl_3$, compared to BSA-treated group (F). Cell-based system demonstrated that treatment of ESI09 (n = 8) weakened plasminogen binding to endothelial surfaces and reduced plasmin generation, compared to vehicle-treated group (n = 8) (G) (*P < 0.05). Carboxypeptidase B (CpB) or ε-aminocaproic acid (ε-ACA) were used as negative controls [8]. HUVECs were transfected with pEGFP-HA vectors expressing full-length ANXA2 before vehicle- or ESI09-treatment. Plasmin activity assay demonstrated that ectopic expression of ANXA2 can attenuate the inhibition of plasmin activity by inactivation of EPAC1 (H) (*P < 0.05).

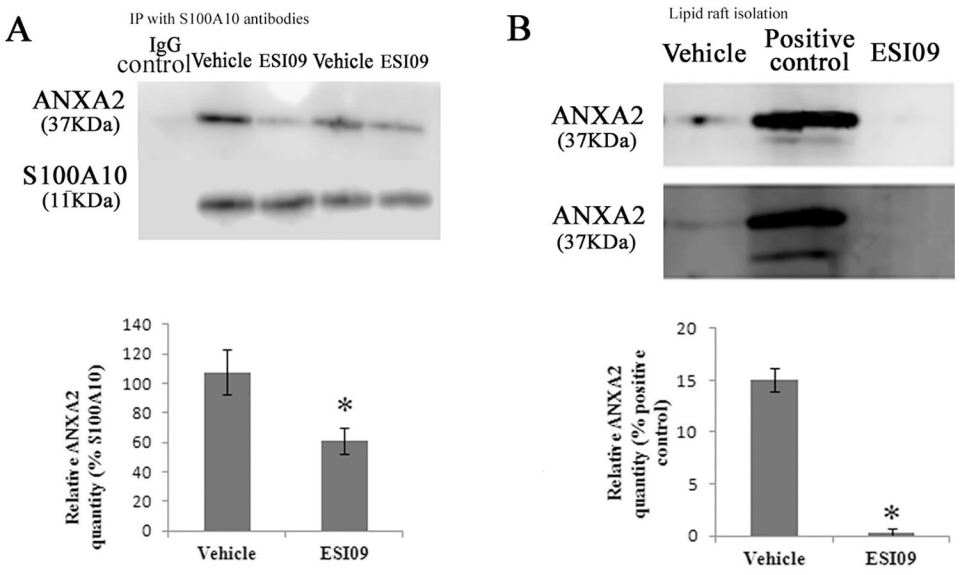

Fig. 4.

Inhibition of EPAC1 interrupts ANXA2 binding to lipid rafts and ANXA2 association with S100A10 in HUVECs. WB shows decreased levels of associated ANXA2 in S100A10 precipitates in ESI09-treated HUVECs (n = 3), compared with vehicle-treated HUVECs (n = 3) (A) ($P < 0.05$). ANXA2 levels were presented as percentages of the indicated loading controls in densitometry. Significantly reduced ANXA2 was detected in lipid rafts from ESI09-treated HUVECs (n = 3), compared with vehicle-treated group (n = 3) (B) ($P < 0.01$). A cell lysate was used as positive control. ANXA2 levels were presented as percentages of the positive controls in densitometry. Equal loading amounts of proteins were confirmed with lipid raft- and non-lipid raft-specific assays (Fig. S7). All experiments were repeated three times.

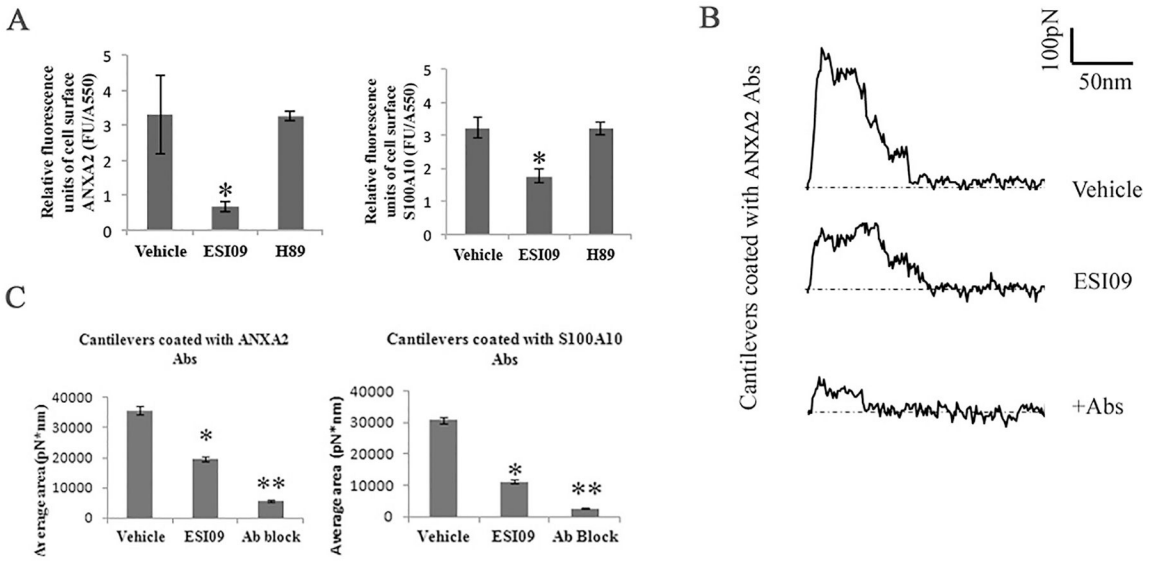

Fig. 5.

Inhibition of EPAC1 impedes ANXA2 and S100A10 residing on endothelial apical surfaces. An impermeable cell-based ELISA assay was employed to compare ANXA2 and S100A10 in ESI09 (5 μM, n = 12)-, H89 (10 μM, n = 12)-, and vehicle-only (n = 12) treated HUVECs (A). Compared with the vehicle-treated group, ESI09-treated HUVECs show lower relative fluorescence units corrected for cell protein (FU/A550) of ANXA2 and S100A10 ($P < 0.05$) signals on the surfaces of HUVECs. The data presented are representative of three independent experiments.

The unbinding work of cell surface antigens with a relevant antibody on a cantilever surface was quantified by force-distance curve-based atomic force microscopy (AFM) (representative curves in B). During static force mode spectroscopy as the cantilever is pulled up from the cell surface, the unbinding force reaches its peak before all antigen–antibody interactions rupture. These specific unbinding force measurements can be compiled for quantification of total ANXA2 or S100A10 expression on selected areas on the HUVEC cell surface (C). With ANXA2 or S100A10 antibody-coated cantilevers, the unbinding work of vehicle-treated HUVECs is higher than that of ESI09-treated HUVECs (*$P < 0.05$, *$P < 0.01$), indicating reduced cell surface ANXA2 and S100A10 expression after ESI09 treatment. Ab block: ANXA2 antibody and S100D10 antibody at 25 μg/ml for 30 min in medium, respectively, before the AFM measurement.

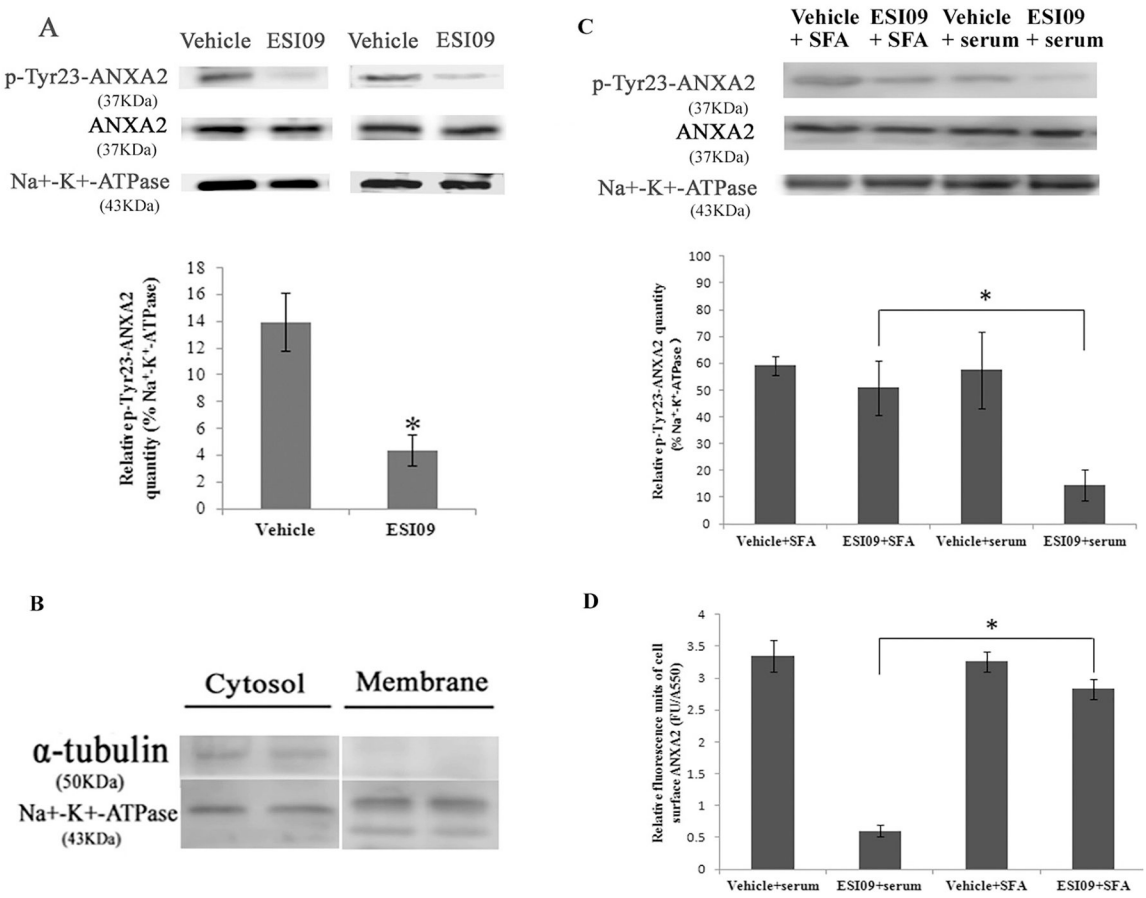

Fig. 6.

Inhibition of EPAC1 decreased tyrosine 23-phosphorylated ANXA2 in the cell membrane compartment. Representative WB (A) shows reduced expression of tyrosine 23-phosphorylated ANXA2 (p-Tyr23-ANXA2) in the membrane fractionation of ESI09-treated HUVECs (n = 4) compared with vehicle-treated HUVECs (n = 4) ($P < 0.05$). Densitometry was used to quantify the relative intensity of tyrosine 23-phosphorylated ANXA2-specific immunoblots normalized by the indicated loading controls. The purity of the isolation of cell membrane proteins was evaluated (B). Representative WB (C, n = 3 for each group) shows restored expression of tyrosine 23-phosphorylated ANXA2 in the membrane fractionation of ESI09-treated Src family activator (SFA)-exposed HUVECs, compared to ESI09-treated HUVECs (* $P < 0.05$). An impermeable cell-based ELISA assay shows increased relative fluorescence units of cell surface ANXA2 in ESI09-treated SFA-exposed HUVECs, compared to ESI09-treated group (D, n = 4 for each group) (*$P < 0.05$). All experiments were repeated three times.

Table 1

$FeCl_3$-induced carotid arterial thrombosis detected in mice.

Group	Pre-treatment	Number of animals	Carotid arterial thrombosis (%)[a]
WT		12	8.33
KO		12	41.67
KO	rANXA2	11	9.09
KO	BSA	5	40
WT	BSA	5	0
WT	rANXA2	4	0

[a]Near-serial cross sections were stained with the use of hematoxylin and eosin to detect thrombus in carotid arteries by bright field microscopy.